Asian Journal of Periodontics and Orthodontics
2025, Volume 5, Page No: 104-12
Copyright CC BY-NC-SA 4.0
Available online at: www.tsdp.net

ISSN: 3062-3499

Original Article

Impact of Pulsed Electromagnetic Field Stimulation on Alveolar Bone Remodeling in Orthodontic Retention: An Experimental Rat Study

Jingyi Qiao[1], Bing Jiang[1], Moude Liu[1]*

[1]Stomatological Materials Laboratory, School of Stomatology, Shandong First Medical University & Shandong Academy of Medical Sciences, Tai'an, Shandong 271016, China.

***E-mail** ✉ Moudelin4@163.com

Received: 17 May 2025; **Revised:** 09 October 2025; **Accepted:** 14 October 2025

ABSTRACT

Retention after orthodontic treatment relies on continuous alveolar bone remodeling to preserve stability. Pulsed electromagnetic field (PEMF) stimulation, widely used in managing bone disorders, may support this process by promoting osteogenesis and limiting resorption. In this study, 36 male Wistar rats were assigned to control, PEMF 7-day, and PEMF 14-day groups. Tooth movement was first induced with nickel–titanium coil springs for 21 days, after which retention was simulated by filling the created space with glass ionomer cement. During retention, experimental groups were exposed daily to PEMF (15 Hz, 2.0 mT, 2 h). Animals were sacrificed at different time points to measure Wnt5a mRNA and the protein levels of RANKL, OPG, ALP, and Runx2 on the tension side. Statistical analysis (ANOVA, $p < 0.05$) revealed that PEMF exposure elevated Wnt5a, OPG, ALP, and Runx2 expression, while suppressing RANKL compared with controls. These findings indicate that PEMF facilitates alveolar bone remodeling during orthodontic retention by enhancing bone formation and reducing bone resorption.

Keywords: Pulsed electromagnetic field, Alveolar bone, Orthodontic retention, Remodeling

How to Cite This Article: Qiao J, Jiang B, Liu M. Impact of Pulsed Electromagnetic Field Stimulation on Alveolar Bone Remodeling in Orthodontic Retention: An Experimental Rat Study. Asian J Periodont Orthodont. 2025;5:104-12. https://doi.org/10.51847/lkiDoddp0Z

Introduction

The stability of orthodontic corrections is closely linked to the biological process of alveolar bone remodeling that occurs during the retention phase. When orthodontic forces are applied, bone resorption typically initiates on the compression side, while bone deposition follows on the tension side to accommodate the new tooth position [1]. A number of molecular pathways and biomarkers regulate this dynamic, including non-canonical Wnt signaling, runt-related transcription factor 2 (Runx-2), receptor activator of nuclear factor kappa B ligand (RANKL), osteoprotegerin (OPG), and alkaline phosphatase (ALP). Wnt5a, for instance, can trigger canonical Wnt signaling, leading to β-catenin migration into the nucleus and activation of osteoblast proliferation [2]. Runx-2 and ALP are widely regarded as markers of osteoblast differentiation and mineralization [3, 4], whereas the RANKL/OPG system maintains equilibrium between bone resorption and deposition [5, 6].

One of the persistent difficulties in orthodontics is preventing relapse, the tendency of teeth to shift back toward their pre-treatment alignment, even after years of retainer use [7]. This underscores the need for supportive strategies that accelerate and stabilize bone remodeling during retention. Among the available noninvasive options, pulsed electromagnetic field (PEMF) therapy has received considerable attention. PEMF has been applied in the management of postmenopausal osteoporosis [8, 9], has been shown to enhance fracture repair and bone formation, and is also effective in reducing pain [10–12]. The U.S. Food and Drug Administration recognizes PEMF as a safe and effective method for clinical bone repair without reported adverse effects [13, 14].

Evidence from cellular studies shows that PEMF promotes osteoblast activity while downregulating osteoclast formation [15, 16]. Animal experiments

© 2025 Asian Journal of Periodontics and Orthodontics

further demonstrate that in osteoporotic rat models, PEMF enhances bone remodeling by stimulating osteoblast and osteoclast proliferation, increasing ALP activity, regulating the RANK/RANKL/OPG pathway, and activating Wnt-related mechanisms [17–20]. In clinical orthodontics, PEMF devices have also been associated with reduced discomfort from appliances, which may contribute to smoother and faster treatment [21–24].

Collectively, prior research suggests that PEMF can stimulate bone deposition and favorably influence alveolar bone remodeling. Yet, its role during orthodontic retention has not been systematically investigated. The present study therefore aims to evaluate the impact of PEMF stimulation on alveolar bone remodeling during the retention phase using a rat model.

Materials and Methods

Experimental animal models

The study protocol was approved by the Ethics Committee of the Faculty of Medicine, Brawijaya University (Approval No. 218/EC/KEPK-S 3/09/2022). Thirty-six male Wistar rats (Rattus norvegicus), aged 12 weeks and weighing 250–300 g, were selected. Each rat was housed individually in a controlled environment maintained at ~23 °C, with unrestricted access to food and water. Animals were monitored daily for general health, and body weights were recorded biweekly, starting one week prior to the experiment. Rats that lost ≥15% of their initial body weight during the study were excluded.

The rats were divided into three groups according to treatment protocol:

Control: Orthodontic appliance applied for 21 days; retention phase of 7 days without PEMF exposure.

PEMF 7: Orthodontic treatment for 21 days; retention phase of 7 days with daily PEMF stimulation.

PEMF 14: Orthodontic treatment for 21 days; retention phase of 14 days with daily PEMF stimulation.

Anesthesia was administered intramuscularly using a mixture of ketamine hydrochloride and xylazine (1:1 ratio) at a concentration of 1 kg/mL.

Orthodontic tooth movement in rat models

Tooth movement was performed using a nickel–titanium closed-coil spring (American Orthodontics, Sheboygan, WI, USA), measuring 0.01 inch in diameter and 5 mm in length. The spring was positioned between the maxillary first molar and incisor to deliver a constant force of 50 gF, inducing mesial bodily movement of the first molar. The appliance remained in place for 21 days, as illustrated in **Figures 1a–1c** [18].

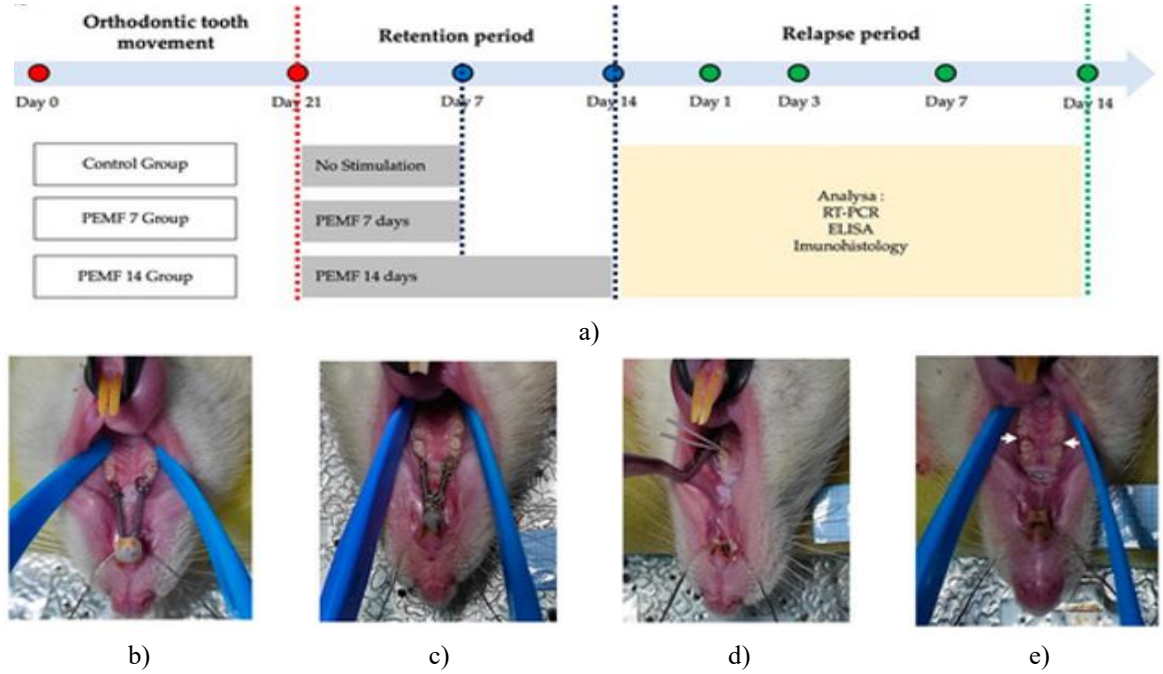


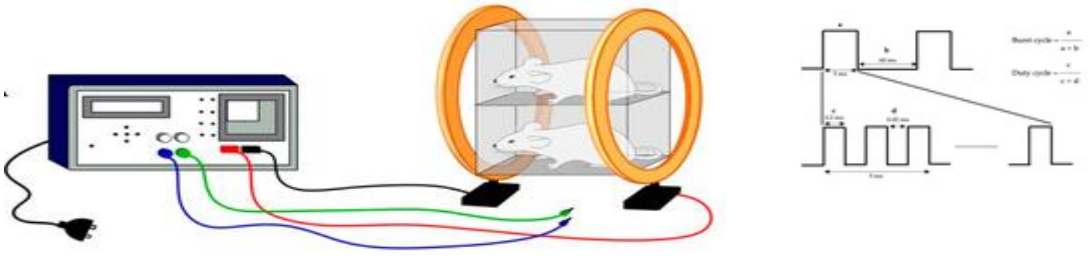
Figure 1. Experimental workflow for the study. Panel (a) illustrates the timing and duration of PEMF exposure. Panel (b) shows the positioning of the orthodontic appliance on the teeth. Panel (c) depicts the dental arrangement after the induced tooth movement. Panel (d) demonstrates the collection of gingival crevicular fluid (GCF) using paper points. Panel (e) indicates the exact site (white arrow) from which samples were obtained for RT-PCR analysis. Abbreviations: PEMF, pulsed electromagnetic field; GCF, gingival crevicular fluid; RT-PCR, real-time polymerase chain reaction.

Retention phase

Following the completion of the 21-day active tooth movement period [25], the retention stage began. The interdental area between the first and second molars was carefully cleared and air-dried. To stabilize the teeth, Fuji type II light-cured glass ionomer cement (GC, Tokyo, Japan) was applied evenly across the space, maintaining alignment with the occlusal surface [26]. After ensuring the cement was properly set, the nickel–titanium closed-coil spring was removed to reduce the risk of immediate relapse.

PEMF exposure

A PEMF stimulator was prepared and fine-tuned following the procedures outlined in previous studies [27–30] **(Figure 2)**. The device produced a square waveform with the following parameters: burst width 5 ms, burst interval 60 ms, pulse width 0.2 ms, pulse interval 0.02 ms, pulse rise 0.3 μs, and pulse fall 2.0 μs. The generated magnetic field reached a peak intensity of 2.0 mT at a repetition rate of 15 Hz [28, 29]. For the retention experiment, rats were individually housed in specialized fiber cages placed on the stimulator platform and exposed to PEMF for two hours daily. The exposure periods were either 7 days (PEMF 7) or 14 days (PEMF 14).



a) b)

Figure 2. Setup for PEMF exposure. a) Rats placed in fiber cages between Helmholtz coils for 2-hour daily PEMF treatment. b) Square waveform details: burst width 5 ms, burst interval 60 ms, pulse width 0.2 ms, pulse interval 0.02 ms, pulse rise 0.3 μs, pulse fall 2.0 μs.

ELISA analysis

After the assigned retention period, the glass ionomer cement was removed. Rats were euthanized on days 1, 3, 7, and 14 to collect samples. Under anesthesia, each rat was positioned on an operating platform, and the mouth was held open with a brace. The gingival surfaces surrounding the first and second molars were cleaned and dried. Sterile #15 paper points were inserted into the distal sulcus of the first molar for 60 seconds to collect gingival crevicular fluid (GCF) **(Figure 1d)**. Each paper point was then transferred to a microcentrifuge tube containing 350 μL phosphate-buffered saline. Samples were centrifuged at 1000×g at 4 °C for 20 minutes, and the supernatants were stored at −80 °C. Concentrations of RANKL, OPG, and ALP were determined using ELISA kits (Rat RANKL: E-EL-R0841; Rat OPG: E-EL-R3005; Rat ALPL: E-EL-R1109; Elabscience, Houston, TX, USA).

RT-PCR-based gene expression analysis

Tissues located distal to the first molar (tension side), comprising periodontal ligament, gingiva, and alveolar bone, were collected for RT-PCR, as shown in **Figure 1e**. Each sample, sized 2 mm × 2 mm, was excised using surgical tools and a low-speed diamond disk, then stored in microcentrifuge tubes at −80 °C. For RNA extraction, samples were ground into a uniform powder using a mortar and pestle. RNA was isolated with an RNAsimple Total RNA Kit (4992858, TIANGEN, Beijing, China) and transcribed into cDNA using a FastKing RT Kit (with gDNase) (Cat. no. 4992223/4992224/4992250; TIANGEN, Beijing, China). Amplification was performed with an HRM Analysis Kit (EvaGreen) (Cat. no. 4992776/4992873, TIANGEN, Beijing, China). Primers for Wnt5a and Beta-actin were designed using the NCBI BLAST Server, with details on sequences, amplicon lengths, melting temperatures, and GenBank accession numbers listed in **Table 1**. Gene expression was quantified relative to Beta-actin via semi-quantitative methods. RT-PCR was conducted using a CFX Opus 96 Real-Time PCR System (Bio-Rad, Hercules, CA, USA) across 40 cycles. The protocol included an initial 120 s denaturation at 95 °C, followed by 10 s denaturation at 95 °C, 20 s annealing at 60 °C, 30 s extension at 72 °C, and a melting curve analysis. Beta-actin served as the internal control, with all experiments performed concurrently under uniform conditions.

Table 1. Primer sequence for RT-PCR analysis.

Target Gene	Primer Type	Primer Sequence (5′–3′)	Amplicon Size (bp)	Melting Temp (°C)	GeneBank ID
Wnt5a	Sense	GCTCGTGGAGTGGTAATGC	148	59.90	NM_022631.3
	Antisense	GCTCGTCCAGAAGTAACAAC		60.04	
Beta-actin	Sense	CCTAAGGCAAACCGTGAGA	152	55.30	NM_017008.4
	Antisense	CAGAGGCATACAGGGACAAC		55.20	

Immunohistochemistry procedures

Once tissues were fixed and decalcified, they were sliced into 3 µm sections. The sections underwent deparaffinization and were then exposed overnight at 4 °C to the primary antibody Runx2 (27-K) (sc-101145, Santa Cruz, Dallas, TX, USA). The next step involved incubation with a secondary enzyme-labeled polymer antibody (N-Histofine High Stain HRP, Nichirei Biosciences Inc., Tokyo, Japan), followed by application of the chromogenic substrate and counterstaining with Mayer's hematoxylin, adhering strictly to the manufacturer's protocol. Runx2-positive osteoblasts were identified as brown-stained cells. For quantification, three separate microscopic areas on the tension side of the alveolar bone were captured at 400× magnification using an Optilab camera. Image analysis was performed with Image G ver. 4.0, and the mean number of positive cells was calculated for each sample.

Statistical analysis

All collected data were evaluated using one-way ANOVA, complemented by post hoc tests, through SPSS software (version 26.0; SPSS Inc., Chicago, IL, USA). A p-value lower than 0.05 was considered indicative of statistical significance.

Results and Discussion

Wnt5a mRNA expression

The relative expression of Wnt5a mRNA was measured using RT-PCR. **Figure 3** demonstrates that both PEMF 7 and PEMF 14 groups exhibited a statistically significant elevation in Wnt5a levels compared with the control group ($p < 0.05$).

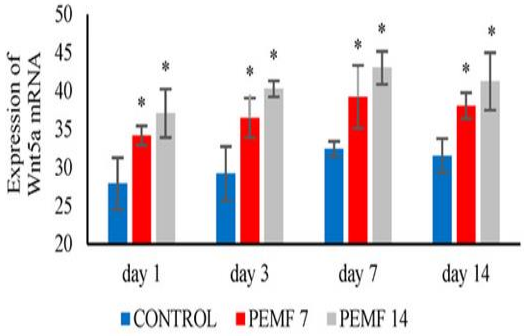


Figure 3. Wnt5a mRNA Quantification**.**
*: $p < 0.05$, indicates a statistically significant difference compared to the control. PEMF: pulsed electromagnetic field.

RANKL, OPG, and ALP profiles

ELISA assessment revealed a reduction in RANKL levels in both the 7-day and 14-day PEMF groups relative to the control cohort. This decrease was statistically significant in the 14-day exposure group ($p < 0.05$), as depicted in **Figure 4**. In contrast, OPG and ALP concentrations increased under PEMF stimulation, with both the 7-day and 14-day PEMF groups showing significant elevations compared to controls ($p < 0.05$). These findings indicate that PEMF may favorably influence bone remodeling by decreasing resorption markers while enhancing bone formation indicators.

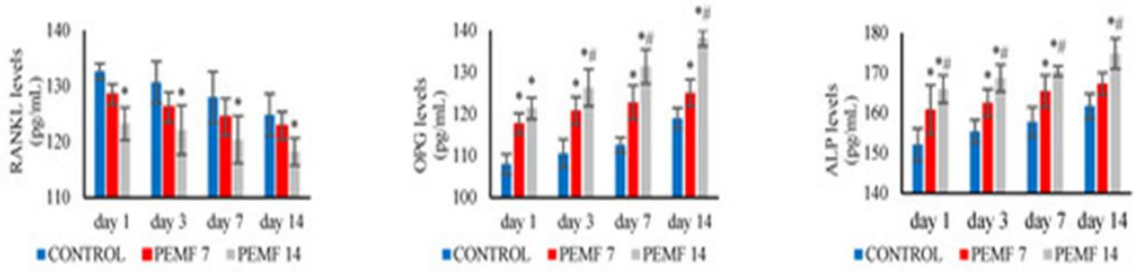


Figure 4. RANKL, OPG, and ALP Concentration Histograms.
*: $p < 0.05$, significant relative to control; #: $p < 0.05$, significant relative to PEMF 7 group. Abbreviations: PEMF – pulsed electromagnetic field; RANKL – receptor activator of nuclear factor-kappa B ligand; OPG – osteoprotegerin; ALP – alkaline phosphatase.

Runx2 expression analysis

Examination of the tension side via immunohistochemistry demonstrated that Runx2-positive osteoblasts were more numerous in PEMF-treated groups than in controls, with significant differences observed for both 7- and 14-day exposures ($p < 0.05$) **(Figure 5)**. The spatial distribution and relative abundance of Runx2-expressing cells in the alveolar bone are illustrated in **Figure 5**, confirming that PEMF exposure promotes osteoblast activity and may support alveolar bone formation during the retention phase.

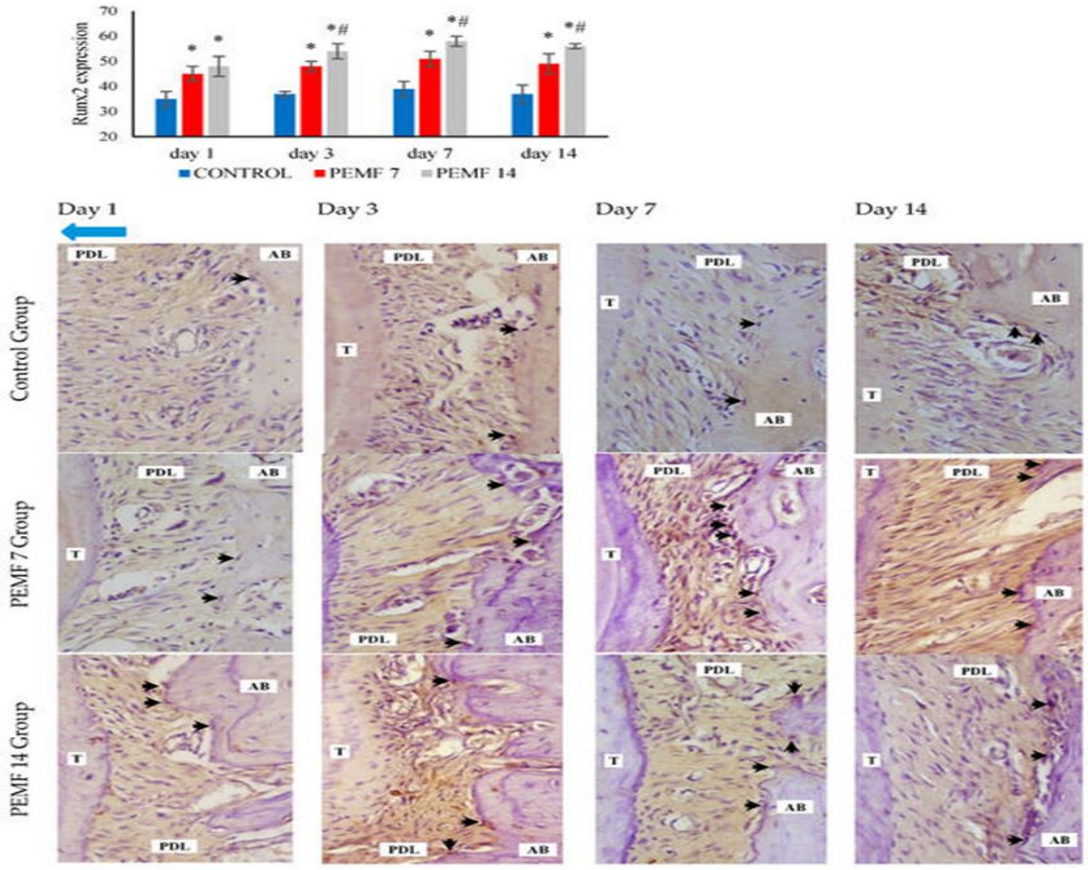


Figure 5. Runx2 Expression: Histogram and Immunohistochemical Images**.** Black arrows indicate Runx2-positive osteoblasts; blue arrows show the direction of tooth movement. *: $p < 0.05$, significant versus control group; #: $p < 0.05$, significant versus PEMF 7 group. Abbreviations: PEMF – pulsed electromagnetic field; T – tooth; PDL – periodontal ligament; AB – alveolar bone; Runx2 – runt-related transcription factor 2.

The retention phase represents the concluding stage of orthodontic therapy, with the primary objective of stabilizing teeth and minimizing the risk of relapse following active orthodontic movement [31]. Relapse can arise from multiple factors, but insufficient remodeling of periodontal tissues is a central contributor. Consequently, the remodeling of alveolar bone is crucial for sustaining post-treatment tooth stability. Findings from the present study demonstrate that exposure to PEMF for 7 and 14 days during the retention phase enhanced bone formation and reduced alveolar bone resorption on the tension side in rat models after orthodontic tooth movement. Supporting evidence from previous investigations indicates that PEMF applied during implant procedures can increase alveolar bone density around implants, thereby improving osteointegration and enhancing implant stability [32].

To investigate the underlying mechanism by which PEMF promotes bone remodeling following orthodontic tooth movement, the non-canonical Wnt5a signaling pathway was analyzed. The data showed an upregulation of Wnt5a mRNA expression on the tension side in both PEMF 7- and 14-day groups. Wnt5a signaling governs the differentiation of bone marrow mesenchymal stromal cells (BMSCs) into mature osteoblasts, inhibits osteoblast apoptosis, and stimulates osteoblast proliferation [33]. Furthermore, Wnt5a enhances the activity of Lrp5 and Lrp6, which are essential for osteoblast differentiation [34]. This pathway plays a significant role in alveolar bone and periodontal ligament remodeling on the tension side

following tooth movement in murine models [35]. Consistent with these findings, previous studies report that PEMF exposure increases bone healing and Wnt5a expression [36].

Additionally, PEMF treatment for both 7 and 14 days led to elevated Runx2 expression on the tension side. Runx2 functions as a key transcription factor guiding the differentiation of mesenchymal cells into osteoblasts and serves as an early indicator of osteogenesis [37]. In line with these observations, Li *et al*. found that PEMF application in type 2 diabetic rats improved bone quality, evidenced by increased Runx2 expression [19]. Similarly, in distraction osteogenesis rat models, PEMF exposure promoted new bone formation, marked by a significant rise in Runx2 gene activity [38]. Moreover, a study using an osteoporotic mouse model reported that four weeks of PEMF stimulation mitigated bone loss and facilitated osteogenic differentiation, indicated by higher Runx2 expression [39].

Following 7 and 14 days of PEMF exposure, ALP and OPG protein levels were significantly elevated, while RANKL levels were reduced. ALP serves as a key biomarker of osteoblast differentiation, particularly in the early phases of osteoblast proliferation, migration, and maturation. The RANKL/OPG signaling pathway regulates osteoclast differentiation and functional activity. These observations align with earlier studies reporting that PEMF stimulation enhances ALP expression [15, 29, 38–42]. RANKL, a membrane-bound protein, interacts with RANK receptors on osteoclasts to promote their differentiation, whereas OPG acts as a decoy receptor, inhibiting osteoclast maturation [43–45]. Thus, PEMF may suppress osteoclastogenesis by modulating the RANK/RANKL/OPG axis. Supporting this, intraperitoneal injection of anti-mRANKL antibodies in rat models undergoing orthodontic tooth movement lowered tartrate-resistant acid phosphatase (TRAP) expression [46]. Zhou *et al*. also demonstrated that PEMF treatment in osteoporotic rats decreased RANKL and increased OPG levels [47], and Catalano *et al*. reported a reduction in the RANKL/OPG ratio following PEMF stimulation in postmenopausal women [9].

In the present study, experimental tooth movement continued for 21 days, followed by retention phases of 7 and 14 days. Prior research examining alveolar bone in adolescent rats with 14 days of molar movement indicated bone deposition, shown by increased bone density and trabecular thickness in both tension and compression areas [48]. Therefore, a 21-day tooth movement period in this rat model can be considered sufficient for complete orthodontic displacement. Biomarkers in the PEMF 14-day group revealed higher Wnt5a mRNA, ALP, and OPG, along with reduced RANKL, compared to the PEMF 7-day group. These findings are consistent with previous studies indicating that a two-week retention phase effectively minimizes orthodontic relapse in experimental models [26].

The present results suggest that PEMF exposure may offer a valuable adjunct in clinical orthodontics by accelerating alveolar bone remodeling during the retention phase, potentially improving treatment stability. Nevertheless, this study is limited to molecular and protein-level analyses; further investigations employing histomorphometry and microCT are necessary to evaluate structural changes in alveolar bone and periodontal tissues post-orthodontic treatment. Additionally, future clinical studies should assess the local and systemic effects of PEMF therapy. Overall, PEMF demonstrates potential as a safe and effective strategy to enhance orthodontic outcomes.

Conclusion

The present study indicates that applying PEMF during the retention phase enhances alveolar bone remodeling following orthodontic tooth movement, particularly on the tension side. A 14-day regimen of PEMF exposure was effective in stimulating alveolar bone formation while reducing bone resorption, likely through modulation of Wnt5a signaling pathways.

Acknowledgments: None

Conflict of Interest: None

Financial Support: None

Ethics Statement: None

References

1. Alikhani M, Sangsuwon C, Al-ansari S, Nervina JM, Teixeira CC. Biphasic theory: breakthrough understanding of tooth movement. J World Fed Orthod. 2018;7(3):82–8.
2. Maeda K, Kobayashi Y, Koide M, Uehara S, Okamoto M, Ishihara A, et al. The regulation of bone metabolism and disorders by Wnt signaling. Int J Mol Sci. 2019;20(22):5525.
3. Aonuma T, Tamamura N, Fukunaga T, Sakai Y, Takeshita N, Shigemi S, et al. Delayed tooth movement in Runx2+/- mice associated with

mTORC2 in stretch-induced bone formation. Bone Rep. 2020;27:100285.
4. Farahani M, Safavi SM, Dianat O, Tusi SK, Younessian F. Acid and alkaline phosphatase levels in GCF during orthodontic tooth movement. J Dent Shiraz Univ Med Sci. 2015;16(3 Suppl):237-45.
5. Shoji-Matsunaga A, Ono T, Hayashi M, Takayanagi H, Moriyama K, Nakashima T. Osteocyte regulation of orthodontic force-mediated tooth movement via RANKL expression. Sci Rep. 2017;7(1):8753.
6. Yang CY, Jeon HH, Alshabab A, Lee YJ, Chung CH, Graves DT. Rankl deletion in periodontal ligament and bone lining cells blocks orthodontic tooth movement. Int J Oral Sci. 2018;10(1):3.
7. Arn ML, Dritsas K, Pandis N, Kloukos D. The effects of fixed orthodontic retainers on periodontal health: a systematic review. Am J Orthod Dentofacial Orthop. 2020;157(2):156-64.
8. Liu HF, Yang L, He HC, Zhou J, Liu Y, Wang CY, et al. Pulsed electromagnetic fields on postmenopausal osteoporosis in Southwest China: a randomized, active-controlled clinical trial. Bioelectromagnetics. 2013;34(4):323-32.
9. Catalano A, Loddo S, Bellone F, Pecora C, Lasco A, Morabito N. Pulsed electromagnetic fields modulate bone metabolism via RANKL/OPG and Wnt/β-catenin pathways in women with postmenopausal osteoporosis: a pilot study. Bone. 2018;116:42–6.
10. Assiotis A, Sachinis NP, Chalidis BE. Pulsed electromagnetic fields for the treatment of tibial delayed unions and nonunions: a prospective clinical study and review of the literature. J Orthop Surg Res. 2012;7(1):24.
11. Shi HF, Xiong J, Chen YX, Wang JF, Qiu XS, Wang YH, et al. Early application of pulsed electromagnetic field in the treatment of postoperative delayed union of long-bone fractures: a prospective randomized controlled study. BMC Musculoskelet Disord. 2013;14(1):35.
12. Mohajerani H, Tabeie F, Vossoughi F, Jafari E, Assadi M. Effect of pulsed electromagnetic field on mandibular fracture healing: a randomized control trial. J Stomatol Oral Maxillofac Surg. 2019;120(5):390-6.
13. Cadossi R, Massari L, Racine-Avila J, Aaron RK. Pulsed electromagnetic field stimulation of bone healing and joint preservation: cellular mechanisms of skeletal response. J Am Acad Orthop Surg Glob Res Rev. 2020;4(5):e1900155.
14. Flatscher J, Pavez Loriè E, Mittermayr R, Meznik P, Slezak P, Redl H, et al. Pulsed electromagnetic fields (PEMF)-physiological response and its potential in trauma treatment. Int J Mol Sci. 2023;24(14):11239.
15. Ferroni L, Gardin C, Dolkart O, Salai M, Barak S, Piattelli A, et al. Pulsed electromagnetic fields increase osteogenetic commitment of MSCs via the mTOR pathway in TNF-α mediated inflammatory conditions: an in-vitro study. Sci Rep. 2018;8(1):5108.
16. He Z, Selvamurugan N, Warshaw J, Partridge NC. Pulsed electromagnetic fields inhibit human osteoclast formation and gene expression via osteoblasts. Bone. 2018;106:194–203.
17. Androjna C, Fort B, Zborowski M, Midura RJ. Pulsed electromagnetic field treatment enhances healing callus biomechanical properties in an animal model of osteoporotic fracture. Bioelectromagnetics. 2014;35(6):396–405.
18. Zhou J, Chen S, Guo H, Xia L, Liu H, Qin Y, et al. Pulsed electromagnetic field stimulates osteoprotegerin and reduces RANKL expression in ovariectomized rats. Rheumatol Int. 2013;33(5):1135-41.
19. Li J, Zeng Z, Zhao Y, Jing D, Tang C, Ding Y, et al. Effects of low-intensity pulsed electromagnetic fields on bone microarchitecture, mechanical strength and bone turnover in type 2 diabetic db/db mice. Sci Rep. 2017;7(1):10834.
20. Jing D, Cai J, Wu Y, Shen G, Li F, Xu Q, et al. Pulsed electromagnetic fields partially preserve bone mass, microarchitecture, and strength by promoting bone formation in hindlimb-suspended rats. J Bone Miner Res. 2014;29(10):2250-61.
21. Jung JG, Park JH, Kim SC, Kang KH, Cho JH, Cho JW, et al. Effectiveness of pulsed electromagnetic field for pain caused by placement of initial orthodontic wire in female orthodontic patients: a preliminary single-blind randomized clinical trial. Am J Orthod Dentofacial Orthop. 2017;152(5):582-91.
22. Mehta SH, Vijayalakshmi D, Kumar NMV, Nagachandran KS. Effectiveness of pulsed electromagnetic field therapy for pain relief in adult patients during the initial space closure phase of orthodontic treatment using sliding mechanics: a single-blind, split-mouth randomized clinical trial. Ann Rom Soc Cell Biol. 2020;24(1):808-28.
23. Dogru M, Akpolat V, Dogru AG, Karadede B, Akkurt A, Karadede MI. Examination of extremely low frequency electromagnetic fields on

orthodontic tooth movement in rats. Biotechnol Biotechnol Equip. 2014;28(1):118-22.
24. Bhad Patil WA, Karemore AA. Efficacy of pulsed electromagnetic field in reducing treatment time: a clinical investigation. Am J Orthod Dentofacial Orthop. 2022;161(5):652-8.
25. Aoki Y, Kako S, Miyazawa K, Tabuchi M, Kimura F, Kataoka K, et al. Dynamics and observations of long-term orthodontic tooth movement and subsequent relapse in C57BL/6 mice. Exp Anim. 2023;72(1):103-11.
26. Qi J, Kitaura H, Shen WR, Kishikawa A, Ogawa S, Ohori F, et al. Establishment of an orthodontic retention mouse model and the effect of anti-c-Fms antibody on orthodontic relapse. PLoS One. 2019;14(6):e0214260.
27. Jiang Y, Gou H, Wang S, Zhu J, Tian S, Yu L. Effect of pulsed electromagnetic field on bone formation and lipid metabolism of glucocorticoid-induced osteoporosis rats through canonical Wnt signaling pathway. Evid Based Complement Alternat Med. 2016;2016(1):4927035.
28. Jing D, Zhai M, Tong S, Xu F, Cai J, Shen G, et al. Pulsed electromagnetic fields promote osteogenesis and osseointegration of porous titanium implants in bone defect repair through a Wnt/β-catenin signaling-associated mechanism. Sci Rep. 2016;6(1):32045.
29. Zhai M, Jing D, Tong S, Wu Y, Wang P, Zeng Z, et al. Pulsed electromagnetic fields promote in vitro osteoblastogenesis through a Wnt/β-catenin signaling-associated mechanism. Bioelectromagnetics. 2016;37(3):152-62.
30. Umiatin U, Dilogo IH, Wijaya SK, Sari P, Djaja AD. Design and development of pulse electromagnetic fields (PEMF) as adjuvant therapy for fracture healing: a preliminary study on rats. AIP Conf Proc. 2019;2092(1):020028.
31. Millett D. The rationale for orthodontic retention: Piecing together the jigsaw. Br Dent J. 2021;230(11):739-49.
32. Adawy M, Darweesh S, Alashwah A, Dessoky N. Effect of pulsed electromagnetic field on the alveolar bone density and its impact on the dental implant osseointegration in osteoporotic patients: A randomized controlled clinical trial. Alex Dent J. 2024;49(1):89–98.
33. Wei X, Liu Q, Guo S, Wu Y. Role of Wnt5a in periodontal tissue development, maintenance, and periodontitis: implications for periodontal regeneration. Mol Med Rep. 2021;23(3):167.
34. Okamoto M, Udagawa N, Uehara S, Maeda K, Yamashita T, Nakamichi Y, et al. Noncanonical Wnt5a enhances Wnt/β-catenin signaling during osteoblastogenesis. Sci Rep. 2014;4(1):4493.
35. Isogai N, Yamaguchi M, Kikuta J, Shimizu M, Yoshino T, Hikida T, et al. Wnt5a stimulates bone formation in tension side during orthodontic tooth movement. Int J Oral Med Sci. 2015;13(3):120-7.
36. Umiatin U, Dilogo IH, Sari P, Wijaya SK. The effect of pulsed electromagnetic field exposure on fracture healing through the Wnt signal pathway. Online J Biol Sci. 2020;20(4):239-49.
37. Gomathi K, Akshaya N, Srinaath N, Moorthi A, Selvamurugan N. Regulation of Runx2 by post-translational modifications in osteoblast differentiation. Life Sci. 2020;245:117389.
38. Li Y, Pan Q, Zhang N, Wang B, Yang Z, Ryaby JT, et al. A novel pulsed electromagnetic field promotes distraction osteogenesis via enhancing osteogenesis and angiogenesis in a rat model. J Orthop Transl. 2020;25(5):87–95.
39. Huang J, Li Y, Zhu S, Wang L, Pei H, Wang X, et al. Pulsed electromagnetic field promotes bone anabolism in postmenopausal osteoporosis through the miR-6976/BMP/Smad4 axis. J Tissue Eng Regen Med. 2023;2023(1):8857436.
40. Bloise N, Petecchia L, Ceccarelli G, Fassina L, Usai C, Bertoglio F, et al. The effect of pulsed electromagnetic field exposure on osteoinduction of human mesenchymal stem cells cultured on nano-TiO2 surfaces. PLoS One. 2018;13(6):e0199046.
41. Liu Y, Hao L, Jiang L, Li H. Therapeutic effect of pulsed electromagnetic field on bone wound healing in rats. Electromagn Biol Med. 2020;40(1):26–32.
42. Kobayashi-Sun J, Kobayashi I, Kashima M, Hirayama J, Kakikawa M, Yamada S, et al. Extremely low-frequency electromagnetic fields facilitate both osteoblast and osteoclast activity through Wnt/β-catenin signaling in the zebrafish scale. Front Cell Dev Biol. 2024;7:1340089.
43. Tsukasaki M, Takayanagi H. Osteoimmunology: evolving concepts in bone-immune interactions in health and disease. Nat Rev Immunol. 2019;19(10):626-42.
44. Ono T, Hayashi M, Sasaki F, Nakashima T. RANKL biology: Bone metabolism, the immune system, and beyond. Inflamm Regen. 2020;40(1):2.
45. Nagy V, Penninger JM. The RANKL-RANK story. Gerontology. 2015;61:534–542.
46. Yoshimatsu M, Kitaura H, Morita Y, Nakamura T, Ukai T. Effects of anti-mouse RANKL antibody

on orthodontic tooth movement in mice. J Dent Sci. 2022;17(3):1087-95.

47. Zhou J, Liao Y, Xie H, Liao Y, Zeng Y, Li N, et al. Effects of combined treatment with ibandronate and pulsed electromagnetic field on ovariectomy-induced osteoporosis in rats. Bioelectromagnetics. 2017;38(1):31–40.
48. Xu B, Yang K. Changes in alveolar bone structure during orthodontic tooth movement in adolescent and adult rats: a microcomputed tomography study. Orthod Craniofac Res. 2023;26(4):568-75.